Design of optimal explicit Runge–Kutta schemes for the high-order spectral difference method

Matteo Parsani

NASA Langley Research Center*

King Abdullah University of Science and Technology

National Institute of Aerosapce
Computational Fluid Dynamics Seminar

April 2, 2013

Acknowledgements

- David Ketcheson (KAUST, KSA)
- Willem Deconinck (ECMWF, UK)
- Michael Bilka (UND, USA)
- Aron Ahamadia (Continuum Analytics, USA)

Low-order methods

A major achievement of the period from 1970 to 1990 was the identification of so called high-resolution shock capturing schemes which are

- non-oscillatory
- second-order accurate almost everywhere
- first-order accurate in the vicinity of extrema

As a result of their favorable properties, the use of low-order schemes has become widespread in both academia and industry, and they form the basis of all commercially available fluid flow solvers.

Low-order methods

Despite these successes, there exists a range of important flow problems (requiring very low numerical dissipation) for which they are not well suited, e.g.,

- vortex dominated flows, e.g.
  - flow around rotor-craft blades
  - flapping wings
- **aeroacoustics**
- **turbulent flows :-)**

It may be advantageous to use a high-order spatial discretizations which offer increased accuracy for a comparable computational cost.

High-order methods

Why high-order accurate methods could outperform the low-orders ones?

- Less dissipative and dissipative on a coarser grids for the same cost than lower-order schemes on finer grids

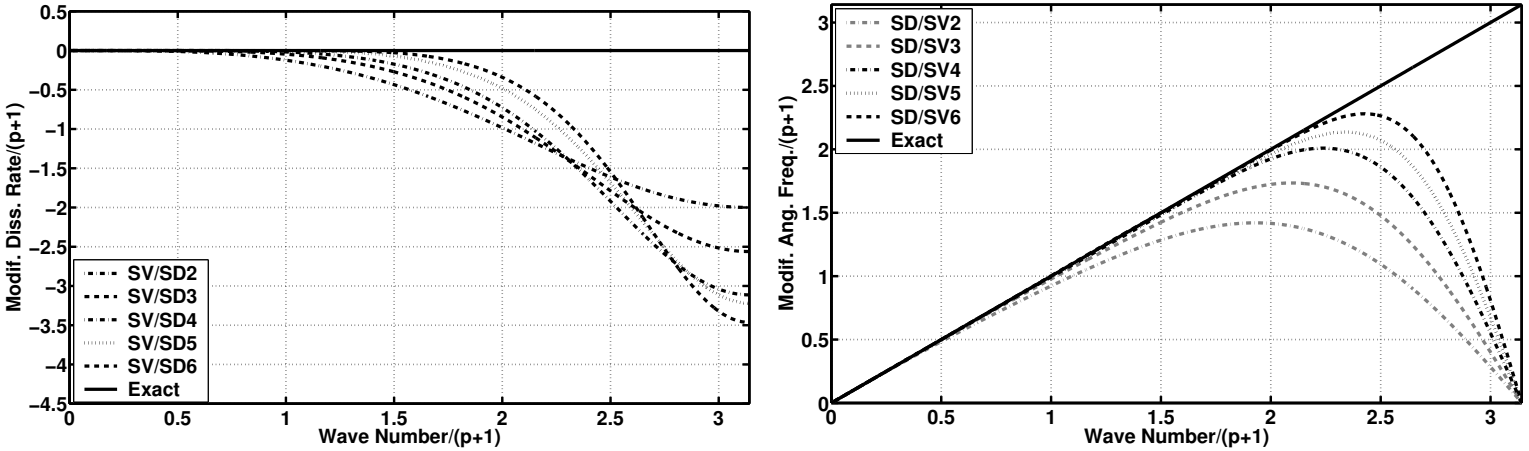

(a) Diffusive properties (b) Dispersive properties

Figure: Example of dispersive and diffusive properties for high-order compact cell-wise continuous polynomials methods.

Considerable effort has been devoted to the development of **compact** spatially **high order** methods on **unstructured** grids for system of PDEs, e.g.

- Discontinuous Galerkin
- Spectral difference
- Spectral volume
- Flux reconstruction
- etc.

Before this era, available high-order methods were designed to be used on Cartesian or very smooth structured curvilinear meshes, e.g. spectral element

Open issues for high-order methods

The use of high-order methods in academia remains limited, and it is practical inexistent in industry.

Reasons:

- lack of robust high-order mesh generation software
- lack of robust and accurate shock capturing algorithms
- (lack of subgrid-scale models)
- **lack of simple and efficient time integration schemes tailored specifically for high-order spatial discretizations**

Spectral difference

- General system of conservation laws in physical space:

$$\frac{\partial \mathbf{q}}{\partial t} + \vec{\nabla} \cdot \left(\vec{\mathbf{f}}_C(\mathbf{q}) - \vec{\mathbf{f}}_D\left(\mathbf{q}, \vec{\nabla}\mathbf{q}\right)\right) = \frac{\partial \mathbf{q}}{\partial t} + \vec{\nabla} \cdot \vec{\mathbf{f}} = 0$$

- Mapped coordinate system on each cell $\rightarrow$

$$\vec{\mathbf{f}}_i^{\vec{\xi}} = \begin{bmatrix} \mathbf{f}_i^{\vec{\xi}} \\ \mathbf{g}_i^{\vec{\xi}} \\ \mathbf{h}_i^{\vec{\xi}} \end{bmatrix} = J_i \vec{\vec{J}}_i^{-1} \begin{bmatrix} \mathbf{f}_i \\ \mathbf{g}_i \\ \mathbf{h}_i \end{bmatrix} = J_i \vec{\vec{J}}_i^{-1} \vec{\mathbf{f}}_i$$

$$\frac{\partial \left(J_i \mathbf{q}_i\right)}{\partial t} \equiv \frac{\partial \mathbf{q}_i^{\vec{\xi}}}{\partial t} = -\frac{\partial \mathbf{f}_i^{\vec{\xi}}}{\partial \xi_1} - \frac{\partial \mathbf{g}_i^{\vec{\xi}}}{\partial \xi_2} - \frac{\partial \mathbf{h}_i^{\vec{\xi}}}{\partial \xi_3} = -\vec{\nabla}^{\vec{\xi}} \cdot \vec{\mathbf{f}}_i^{\vec{\xi}}$$

Spectral difference

- Solution (degree p) and flux polynomials (degree $p+1$):

$$\mathbf{q}_i \approx \mathbf{Q}_i\left(\vec{\xi}\right) = \sum_{j=1}^{N^s} \mathbf{Q}_{i,j}\, L_j^s\left(\vec{\xi}\right), \qquad \vec{\mathbf{F}}_i^{\vec{\xi}}\left(\vec{\xi}\right) = \sum_{l=1}^{N^f} \vec{\mathbf{F}}_{i,l}^{\vec{\xi}}\, L_l^f\left(\vec{\xi}\right)$$

$$\frac{d\mathbf{Q}_{i,j}}{dt} = -\frac{1}{J_{i,j}}\, \vec{\nabla}^{\vec{\xi}} \cdot \vec{\mathbf{F}}_i^{\vec{\xi}}\Big|_j = \mathbf{R}_{i,j}$$

- Riemann flux to handle the solution discontinuity.

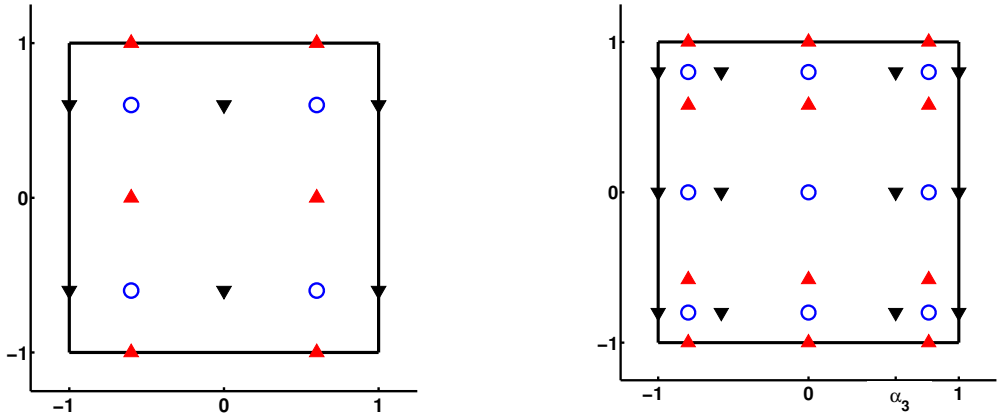

(a) $p = 1$. (b) $p = 2$.

Model problem

2D linear advection equation: $\frac{\partial q}{\partial t} + \vec{\nabla} \cdot (\vec{a} q) = 0$

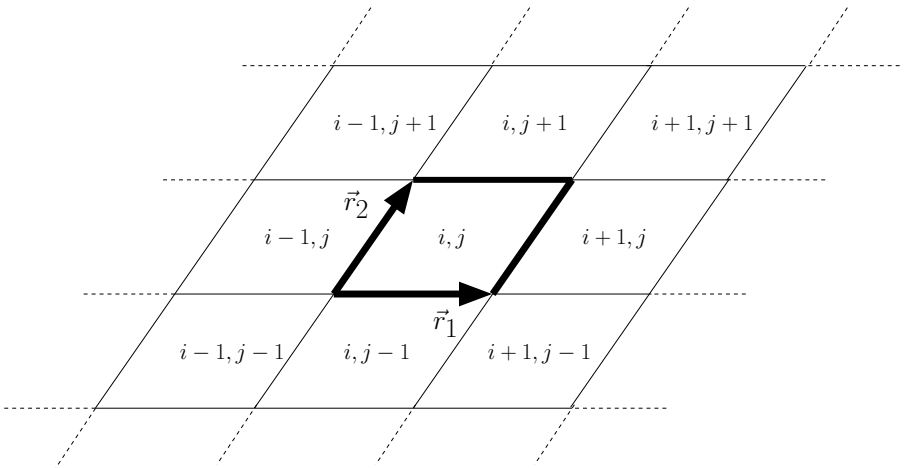

Figure: Generating pattern.

Insert Fourier wave: $\mathbf{Q}_{i,j}(t) = \tilde{\mathbf{Q}}(t) e^{I\vec{k}\cdot\left(i\vec{r}_1{}' + j\vec{r}_2{}'\right)\Delta r} = \tilde{\mathbf{Q}}(t) e^{I\vec{K}\cdot\left(i\vec{r}_1{}' + j\vec{r}_2{}'\right)}$

$$\rightarrow \frac{d\tilde{\mathbf{Q}}}{dt} + \frac{|\vec{a}|}{\Delta r}\mathbf{L}\tilde{\mathbf{Q}} = 0, \quad \Delta r = |\vec{r}_1|$$

Why lack of efficient time integrations?

- It is desirable to use the largest step size possible if the temporal discretization error is acceptable.
- For higher order schemes, the spectrum of the Jacobian of the semi-discretization often has increasingly large eigenvalues.

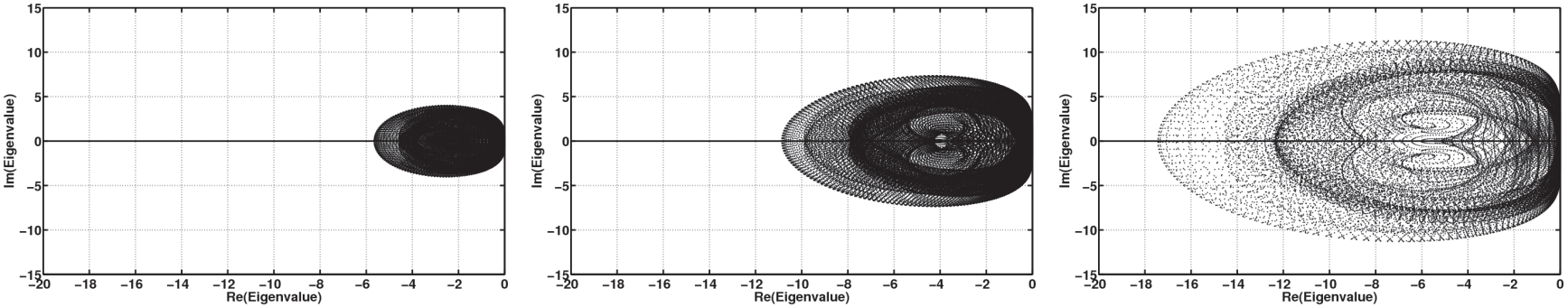

(a) 2nd-order SD (b) 3rd-order SD (c) 4th-order SD

Figure: Fourier footprint of the 2D advection equation.

Time integration schemes for high-order methods

- For explicit time stepping schemes the step size is often limited by stability requirements, which become stricter with higher order methods
- Implicit methods allow the use of much larger step sizes, but lead to very large memory requirements that may not be feasible
- The development of efficient algebraic solvers for high-order implicit discretizations remains challenging

Goal

$\Longrightarrow$ **Explicit time integration methods that allow large step sizes and require less memory seem to be an appealing alternative**

Consider a Runge-Kutta method with Butcher's pair $(\mathbf{A}, \mathbf{b})$,

$$y_i = u_n + \Delta t \sum_{j=1}^{s} a_{ij} f(y_j) \quad (1 \leq i \leq s),$$

$$u^{n+1} = u_n + \Delta t \sum_{j=1}^{s} b_j f(y_j).$$

By applying such a method to the following linear, constant-coefficient IVP

$$\mathbf{Q}'(t) = \mathbf{L}\mathbf{Q}, \quad \mathbf{Q}(t) : \mathbb{R} \to \mathbb{R}^N, \mathbf{L} \in \mathbb{R}^{N \times N},$$
$$\mathbf{Q}(0) = \mathbf{Q}^0,$$

the following iteration is obtained:

$$\mathbf{Q}^{n+1} = \psi(\Delta t \mathbf{L})\mathbf{Q}^n, \quad \psi(z) = 1 + \sum_{j=0}^{s} \mathbf{b}^T \mathbf{A}^{j-1} \mathbf{e}\, z^j,$$

Assume that $\mathbf{L}$ is diagonalizable with eigenvalues let $\lambda_i, i = 1, \ldots, N$. Then the solution is absolutely stable for the time step Δt if

$$\Delta t \lambda_i \in \{z \in \mathbb{C} : |\psi(z)| \leq 1\} \quad \text{for } 1 \leq i \leq N.$$

- if $\mathbf{L}$ is non-normal (i.e. if $\mathbf{L}^* = \mathbf{L}^\top$ does not hold) its pseudospectrum is used

Stability function of explicit Runge–Kutta methods

For an s-stage, order p explicit Runge–Kutta method

$$\psi(z) = \sum_{j=0}^{s} \beta_j z^j = \sum_{j=0}^{p} \frac{1}{j!} z^j + \sum_{j=p+1}^{s} \beta_j z^j$$

Since the exact solution of the IVP is

$$\mathbf{Q}(t) = \exp(t\mathbf{L})\mathbf{Q}^0$$

if the method is accurate to order p, the stability polynomial must be identical to the Taylor expansion of the exponential function up to terms of at least order p.

Design of optimal stability polynomials

- We are interested in designing RK methods that maximize the step size (or $\nu = |\vec{a}| \frac{\Delta t}{\Delta r}$) for which the given stability constraints are satisfied
- In general, the cost of taking a time step is proportional to the number of stages s
- We use the *effective step size* $\Delta t/s$ to compare the computational efficiency of methods with different numbers of stages

Design of optimal stability polynomials

Design optimal methods by first choosing the coefficients β_j to maximize the linearly stable time step

$$\psi(z) = \sum_{j=0}^{p} \frac{1}{j!} z^j + \sum_{j=p+1}^{s} \beta_j z^j$$

Problem (Natural $\psi(z)$ optimization, $\frac{d\tilde{\mathbf{Q}}}{dt} + \frac{|\vec{a}|}{\Delta r}\mathbf{L}\tilde{\mathbf{Q}} = 0$)

Given a spectrum $\{\lambda_i\}$, an order p, and a number of stages s,

$$\begin{aligned} &\textit{maximize} && \nu \\ &\textit{subject to} && |\psi(\nu\lambda_i)| - 1 \leq 0, \;\; i = 1, \ldots, N \end{aligned}$$

Design of optimal stability polynomials

If instead, we assume ν is fixed, we can consider:

Problem (Smart $\psi(z)$ optimization)

Given a spectrum $\{\lambda_i\}$, an order p, and a number of stages s,

$$\textit{minimize} \quad max|\psi(\nu\lambda_i)| - 1 \leq 0, \;\; i = 1, \ldots, N$$

Where we minimize over the coefficients β_j and the maximum is taken over all eigenvalues in the spectrum.

- **Convex feasibility problem, and therefore computationally efficient to solve**
- **Solve a sequence of convex feasibility problems to find the largest ν for which the spectrum lies within a stability polynomial for that step size**

Example of optimal 4th-order ERK scheme

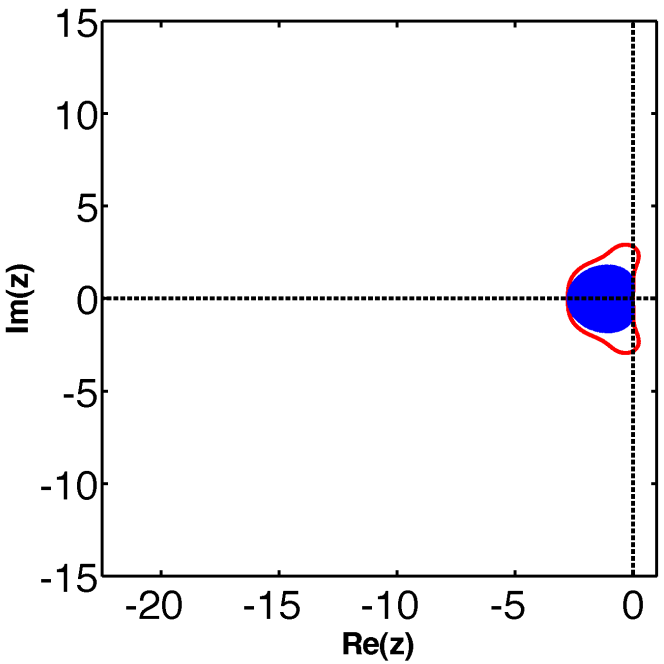

(a) Kutta's ERK(4,4)

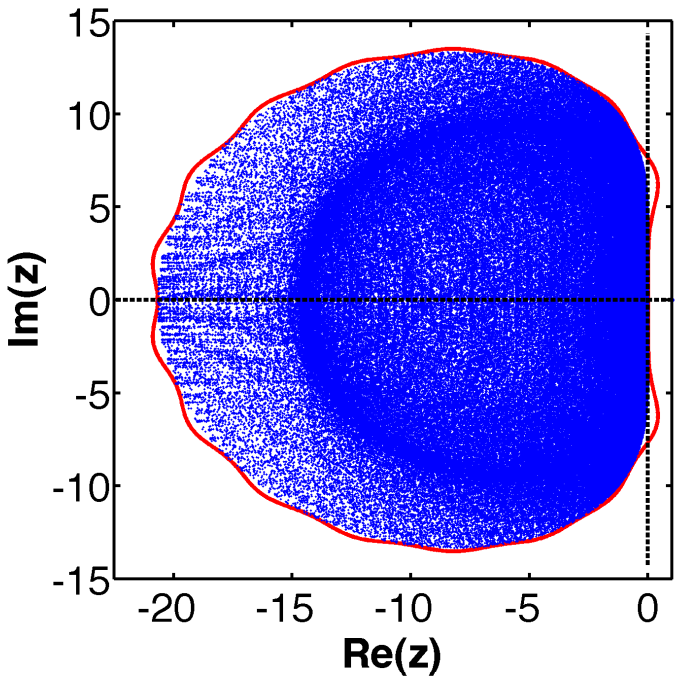

(b) Optimal ERK(18,4)

Effective CFL number (ν_{stab}/s)

- Kutta's ERK(4,4): 3.9534×10^{-2}
- Optimal ERK(18,4): 6.5233×10^{-2} (65% improvement!)

Low storage Runge–Kutta methods

The optimal stability polynomial does not uniquely define the Butcher coefficients:

- Find the Butcher pair $\mathbf{A}, \mathbf{b}$ which minimizes the truncation error coefficients $C^{(p+1)}$, satisfies the order conditions $\tau_i^{(j)}(\mathbf{A}, \mathbf{b}) = 0, (0 \leq j \leq p)$ and can be written in low-storage form with 3 registers $\Gamma(\mathbf{A}, \mathbf{b}) = 0$.

Problem ($C^{(p+1)}(\mathbf{A}, \mathbf{b})$ optimization)

$$
\begin{aligned}
&\textit{minimize} \quad C^{(p+1)}(\mathbf{A}, \mathbf{b}) > 0 \\
&\text{subject to} \\
&\qquad \tau_i^{(j)}(\mathbf{A}, \mathbf{b}) = 0 \qquad (0 \leq j \leq p) \\
&\qquad \Gamma(\mathbf{A}, \mathbf{b}) = 0 \\
&\qquad \mathbf{b}^T \mathbf{A}^{j-1} \mathbf{e} = \beta_j \qquad (0 \leq j \leq s)
\end{aligned}
$$

Stability and accuracy efficiencies

- If the stability is the more restrictive concern, the relative efficiency of two RK methods of order p can be measured as

$$\chi_{\text{stab}} = \frac{\sigma\, \nu_1 / s_1}{\sigma\, \nu_2 / s_2} = \frac{\nu_1 / s_1}{\nu_2 / s_2}$$

  σ: safe factor.

- If the accuracy is the more restrictive concern, the relative efficiency is given by

$$\chi_{\text{acc}} = \left(\frac{C_2^{(p+1)}}{C_1^{(p+1)}} \right)^{\frac{1}{p}} \frac{s_2}{s_1}$$

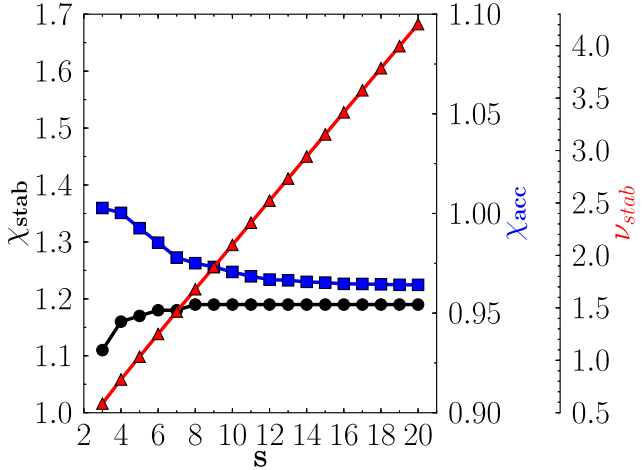

(a) Opt. 2nd-order vs. ERK(2,2)

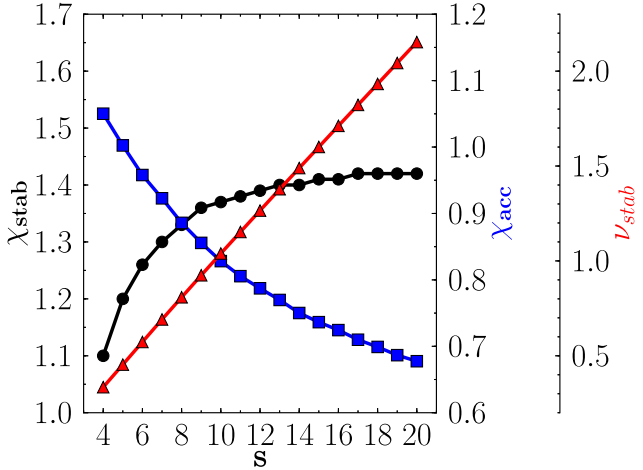

(b) Opt. 3rd-order vs. ERK(3,3)

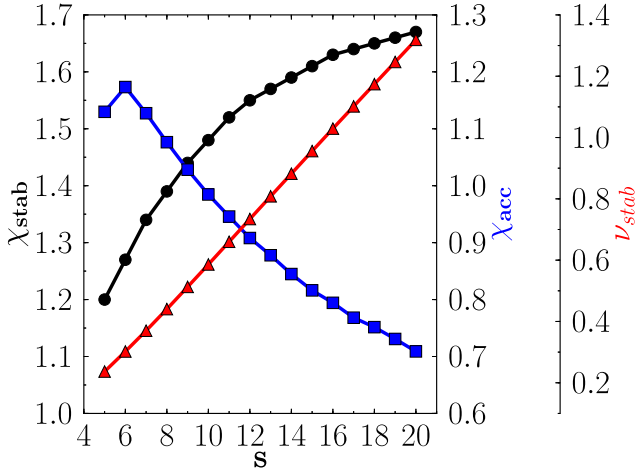

(c) Opt. 4th-order vs. ERK(4,4)

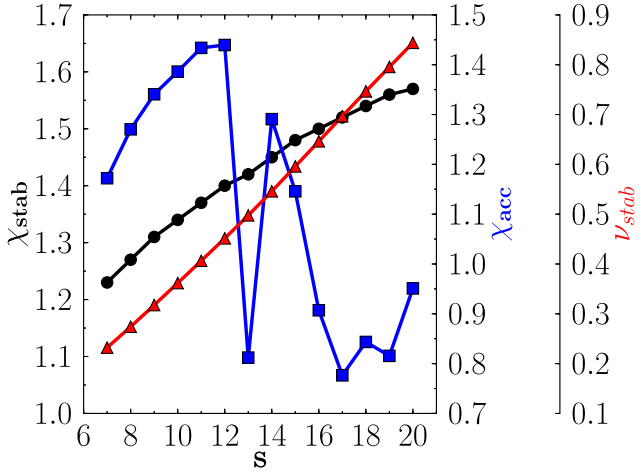

(d) Opt. 5th-order vs. ERKF(6,5)

Figure: Efficiencies and maximum linearly stable CFL number.

Internal stability

In the application of ERK schemes with many stages to time-dependent PDEs, there can be a serious accumulation of errors that may even render methods unusable.

$$\begin{aligned}\epsilon^{n+1} &= \left(v_{s+1} + (\alpha_{s+1} + z\beta_{s+1})\,(I - \alpha_{1:s} - z\beta_{1:s})^{-1}\, v_{1:s}\right)\epsilon^n \\ &+ (\alpha_{s+1} + z\beta_{s+1})\,(I - \alpha_{1:s} - z\beta_{1:s})^{-1}\,\tilde{r} \\ &= P(z)\epsilon^n + \mathbf{Q}(z)\tilde{r}.\end{aligned} \tag{1}$$

Linear advection equation with variable velocity

The conservation law reads

$$\frac{\partial q}{\partial t} + \vec{u} \cdot \vec{\nabla} q = 0, \vec{u}(x, y) = \begin{bmatrix} u \\ v \end{bmatrix} = \omega \begin{bmatrix} -y \\ x \end{bmatrix}$$

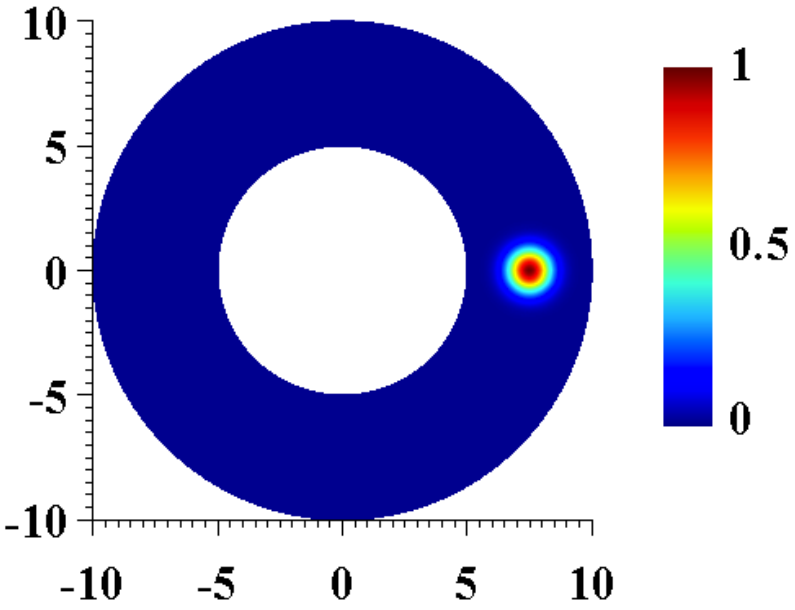

Figure: Gaussian wave advected in an annulus; 4th-order SD method and optimal ERK(18,4) scheme.

Linear advection equation with variable velocity

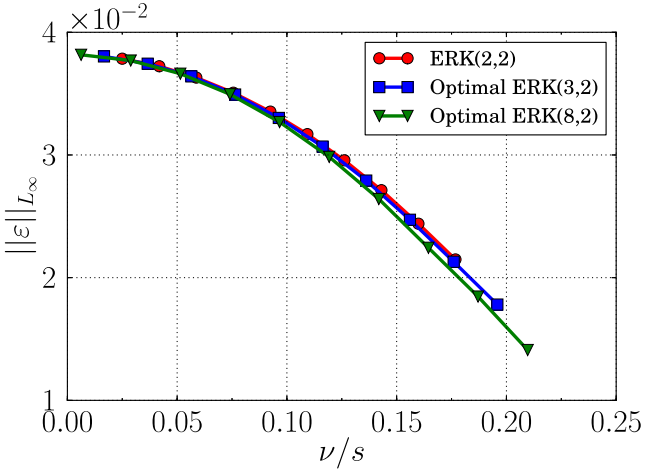

(a) Optimal 2nd-order vs. ERK(2,2)

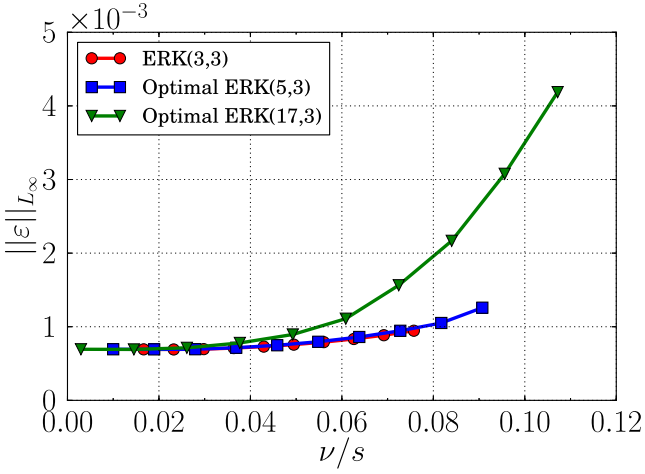

(b) Optimal 3rd-order vs. ERK(3,3)

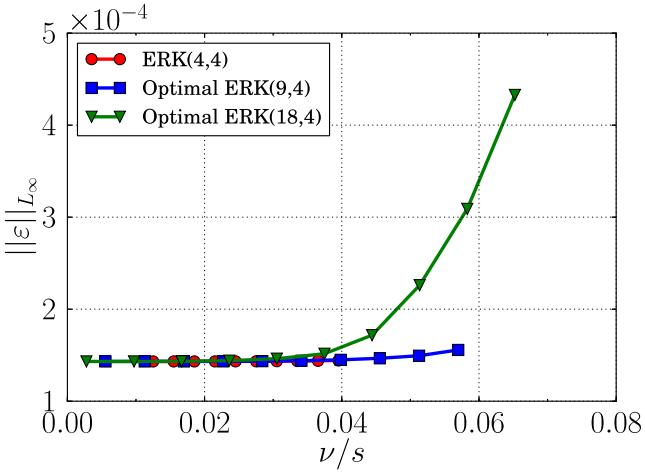

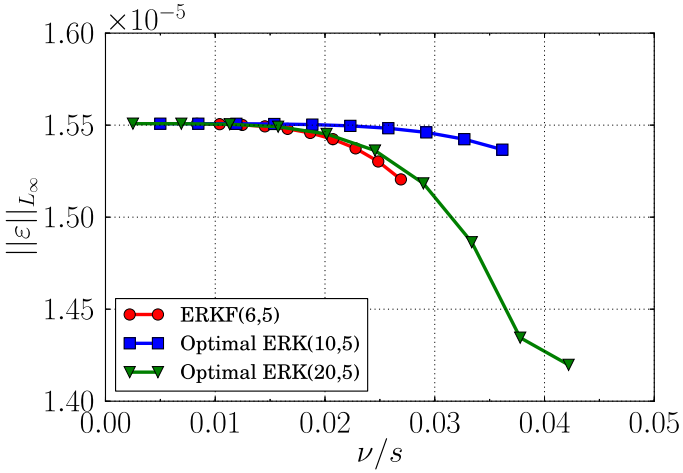

Linear advection equation with variable velocity

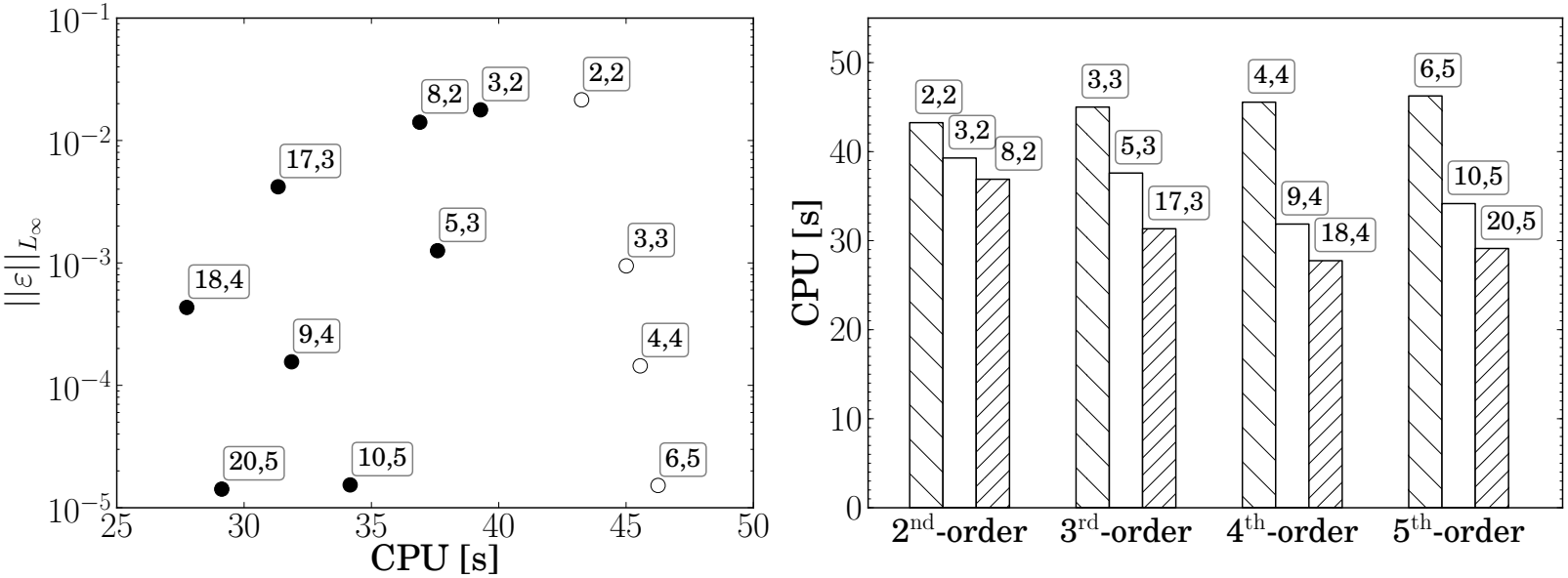

(a) Error versus CPU time. (b) CPU time for each simulation.

Figure: Error and CPU time for the advection problem.

- **Unit increment of the order of accuracy $\rightarrow$ reduction of the error of one order of magnitude**
- **New ERK schemes:** 42% **to** 65% **more efficient for 4th- and 5th-order schemes**

Linearized Euler Equations

Propagation of an acoustic pulse:

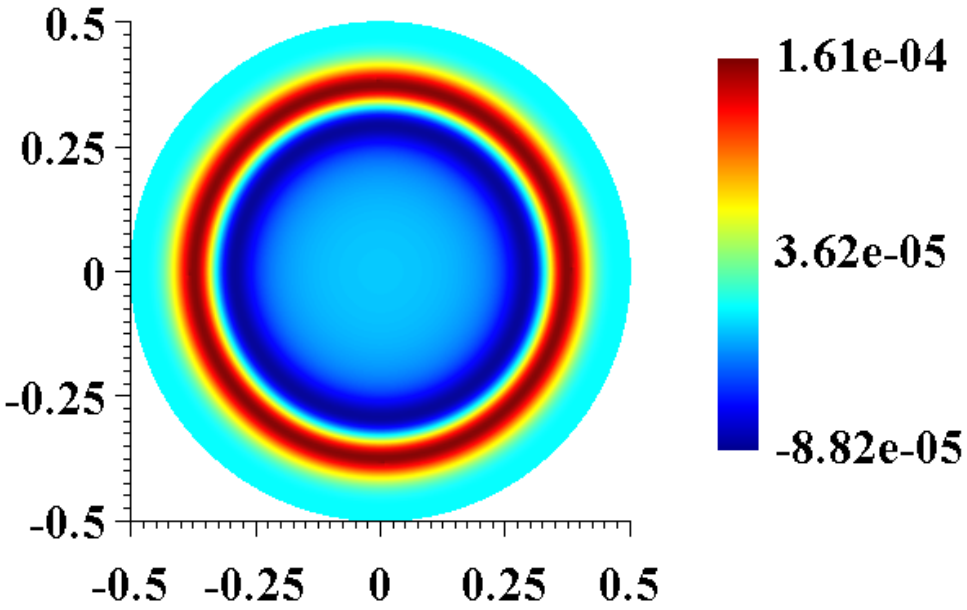

Figure: Propagation of a Gaussian pulse; 4th-order SD method and optimal ERK(18,4) scheme.

Linearized Euler Equations

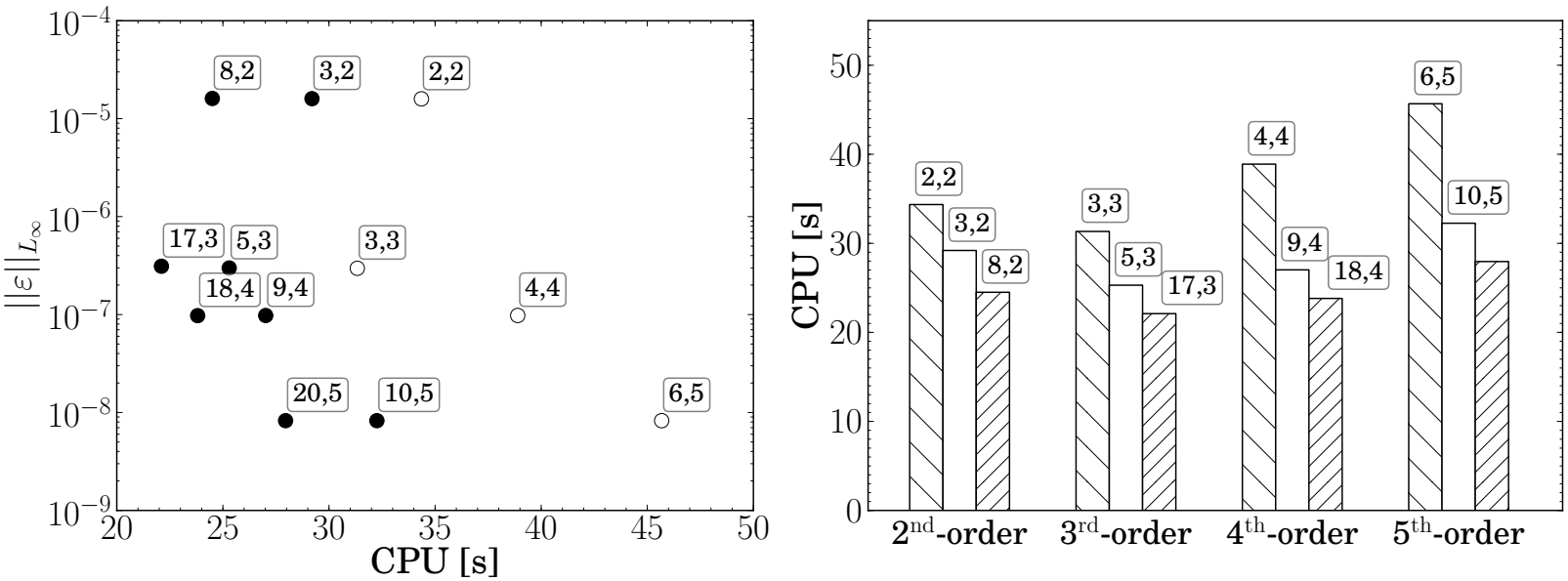

(a) Error versus CPU time.

(b) CPU time for each simulation.

Figure: Error and CPU time for the acoustic pulse problem.

2D compressible Euler Equations

Flow past a wedge:

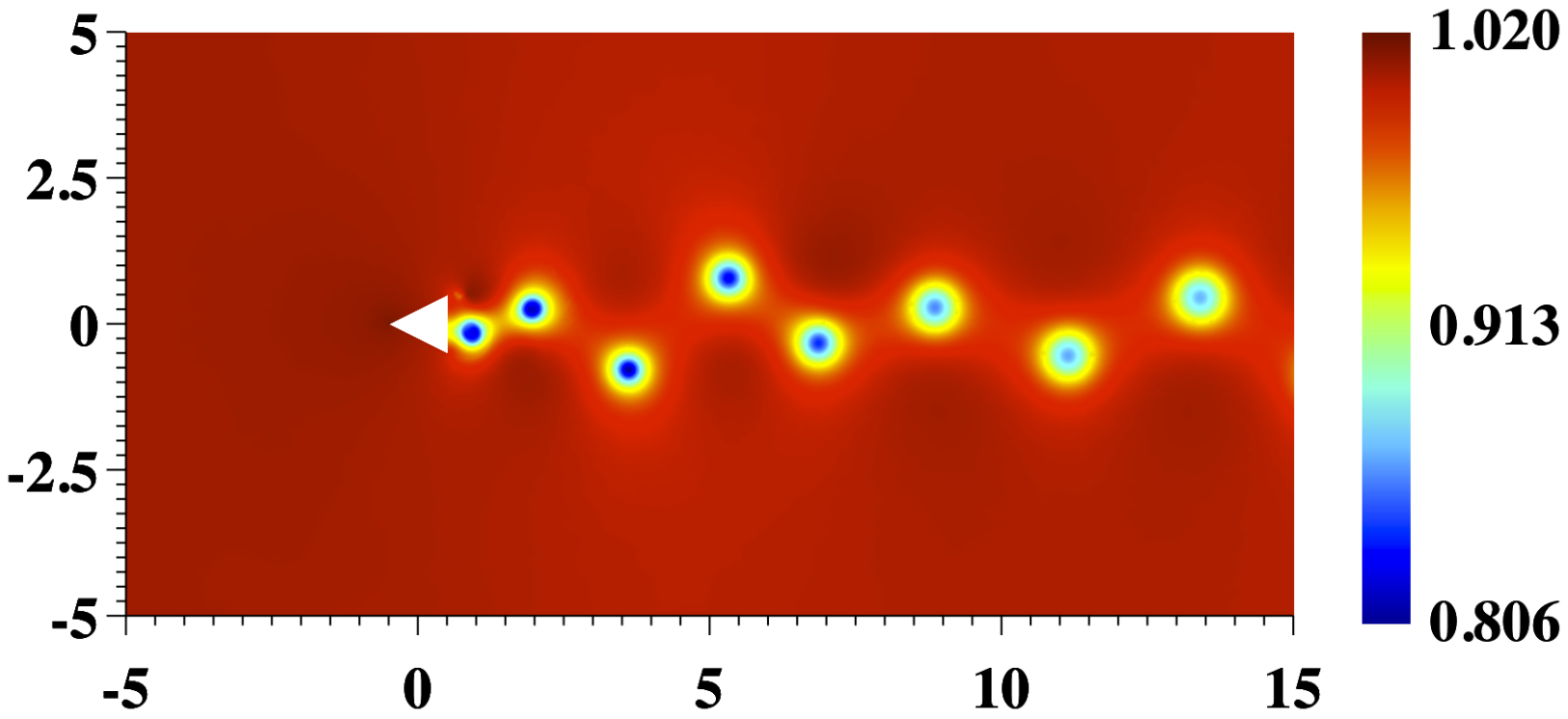

Figure: Density contour of the flow past a wedge; 4th-order SD method and optimal ERK(18,4) scheme.

Compressible Euler Equations

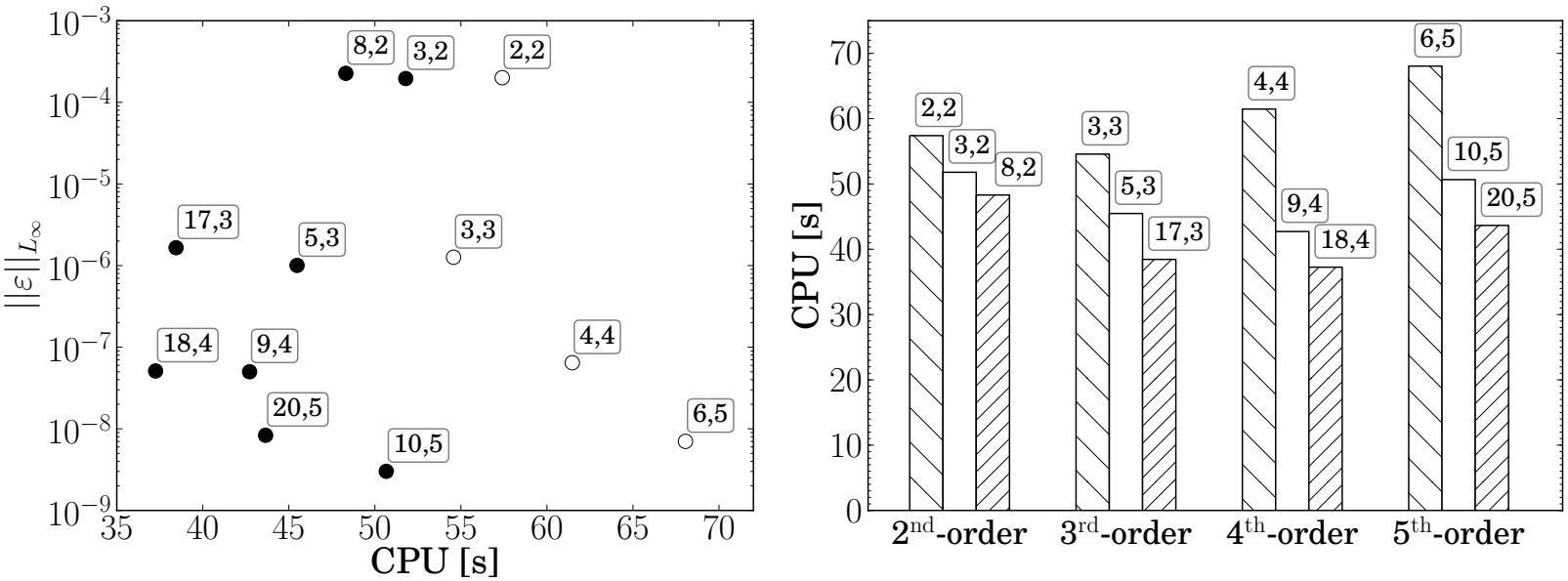

(a) Error versus CPU time. (b) CPU time for each simulation.

Figure: Error and CPU time for the wedge problem.

Optimization of ERK methods for high aspect ratio

We are extending the previous approach to optimize ERK schemes for unstructured grids with aspect ratio (AR) $>> 1$

- AR from 10 to 500 (for now)
- Rectangular domain with periodic and Dirichlet BC for the 2D advection diffusion equation

2D laminar cavity flow

- $Re_\infty = 1500$
- $M_\infty = 0.15$

Evolution of the drag coefficient, C_D vs. *time*:

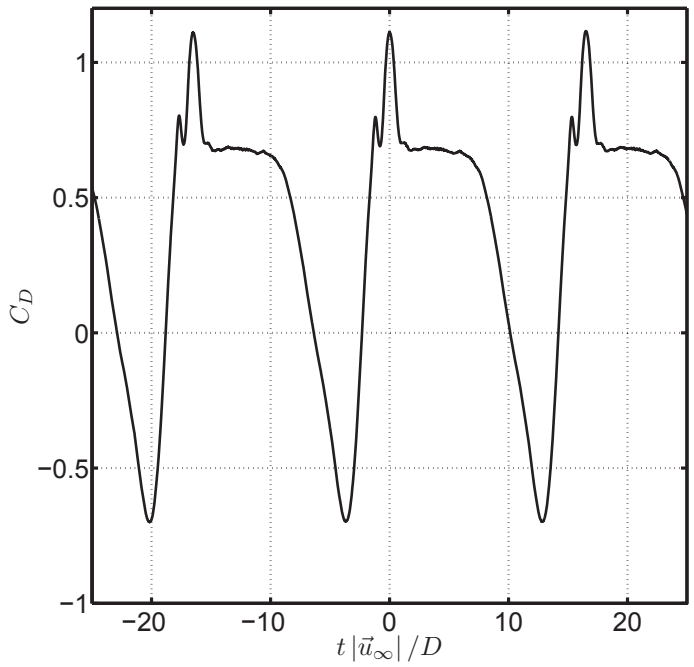

Solution	St	$\langle C_D \rangle$	$\langle C_D^P \rangle$
DNS (Larsson et al.)	0.243	0.377	0.402
SD $p = 2$ (104, 274 DOFs)	0.246	0.385	0.409
SD $p = 3$ (185, 376 DOFs)	0.243	0.379	0.403

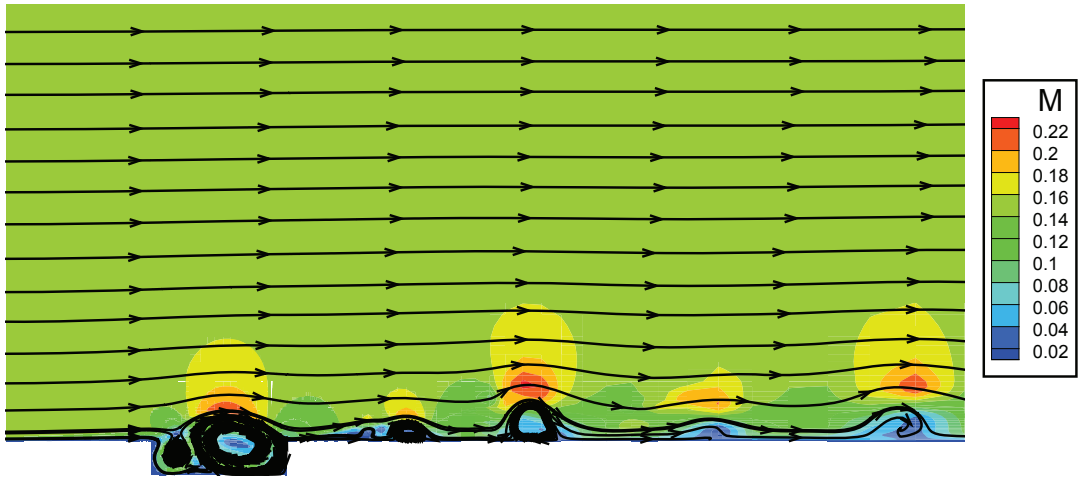

2D laminar cavity flow

Radiated sound field simulation:

- Nine observer points
- Solution for one flow period (laminar flow)
- FW-H approach

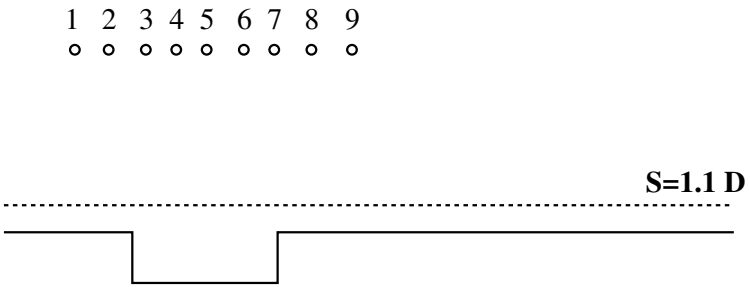

$3rd - order$ SD scheme, 43% speed-up

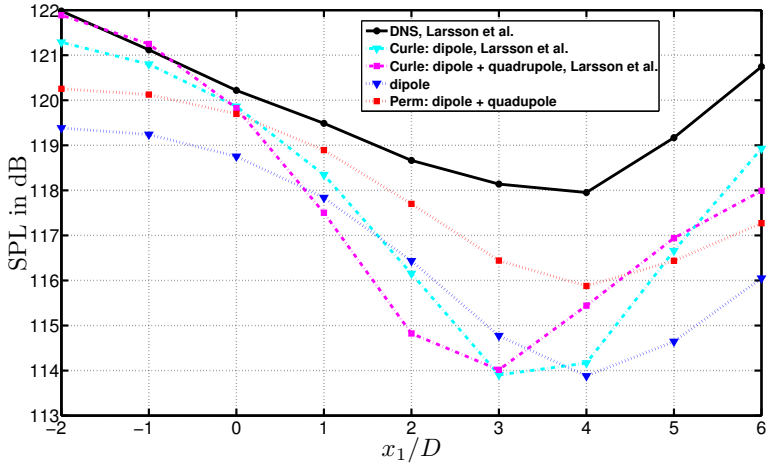

$4th - order$ SD scheme, 62% speed-up

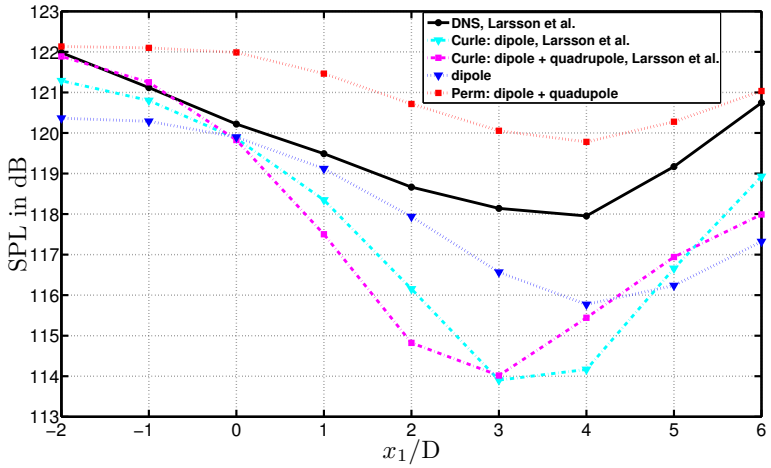

Flow in a muffler

Test case settings:

- $Re_d = 4.64 \times 10^4$, $M = 0.05$, $Pr = 0.72$
- 3D N-S equations and WALE model
- Mesh with $36,612$ hexahedral elements
- $4th$-order SD schemes (2.3×10^6 DOFs; the same used at VKI)
- $CFL \approx 0.7$

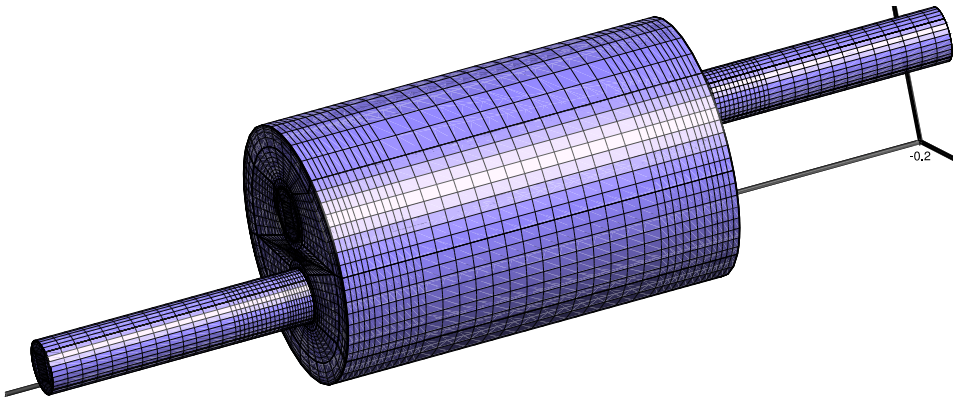

Figure: 3D muffler.

Two preliminary results:

- $\sim 50\%$ speed-up
- Influence of SGS models (?)

Flow in a muffler

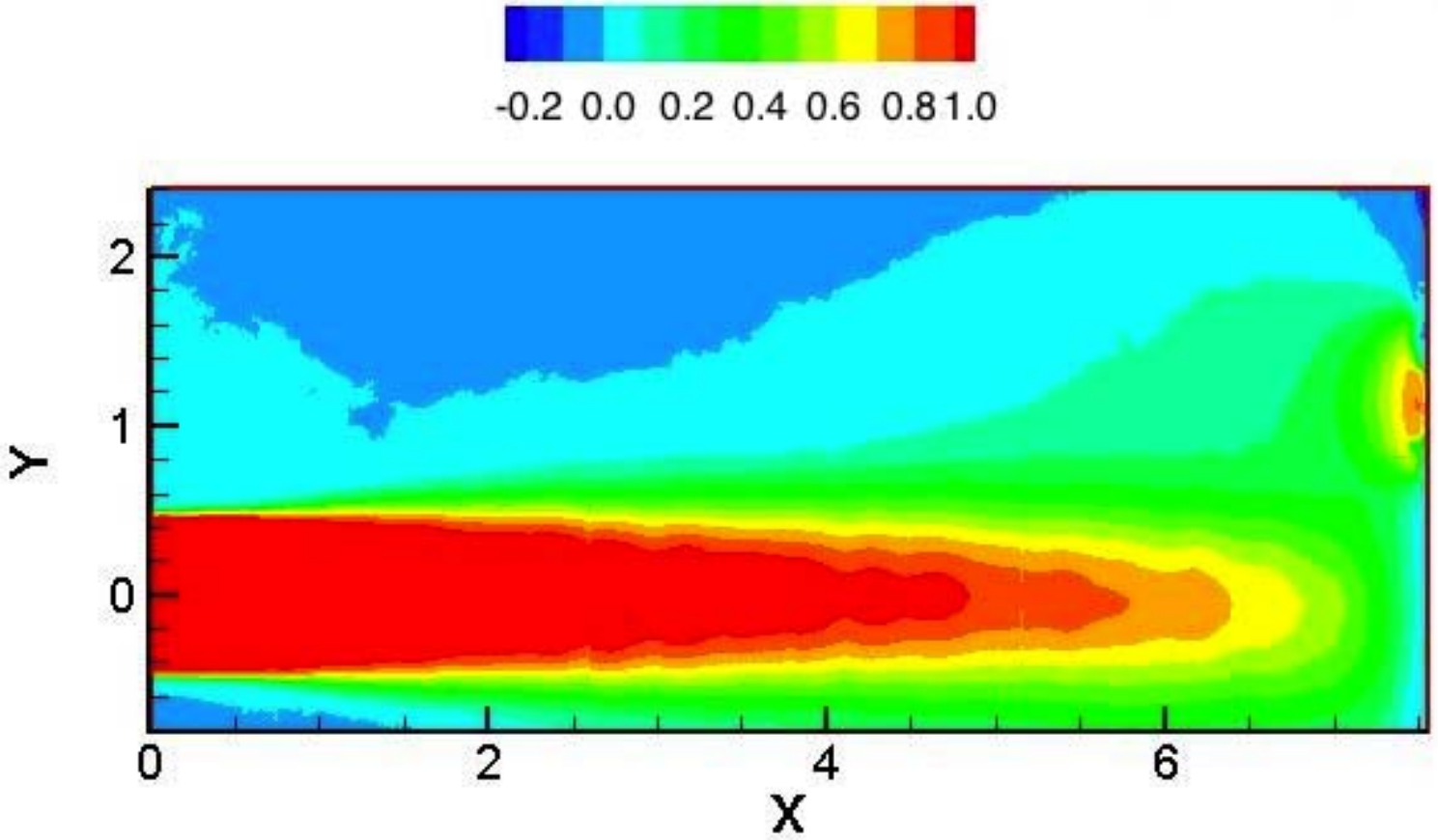

Figure: Average u velocity

Flow in a muffler

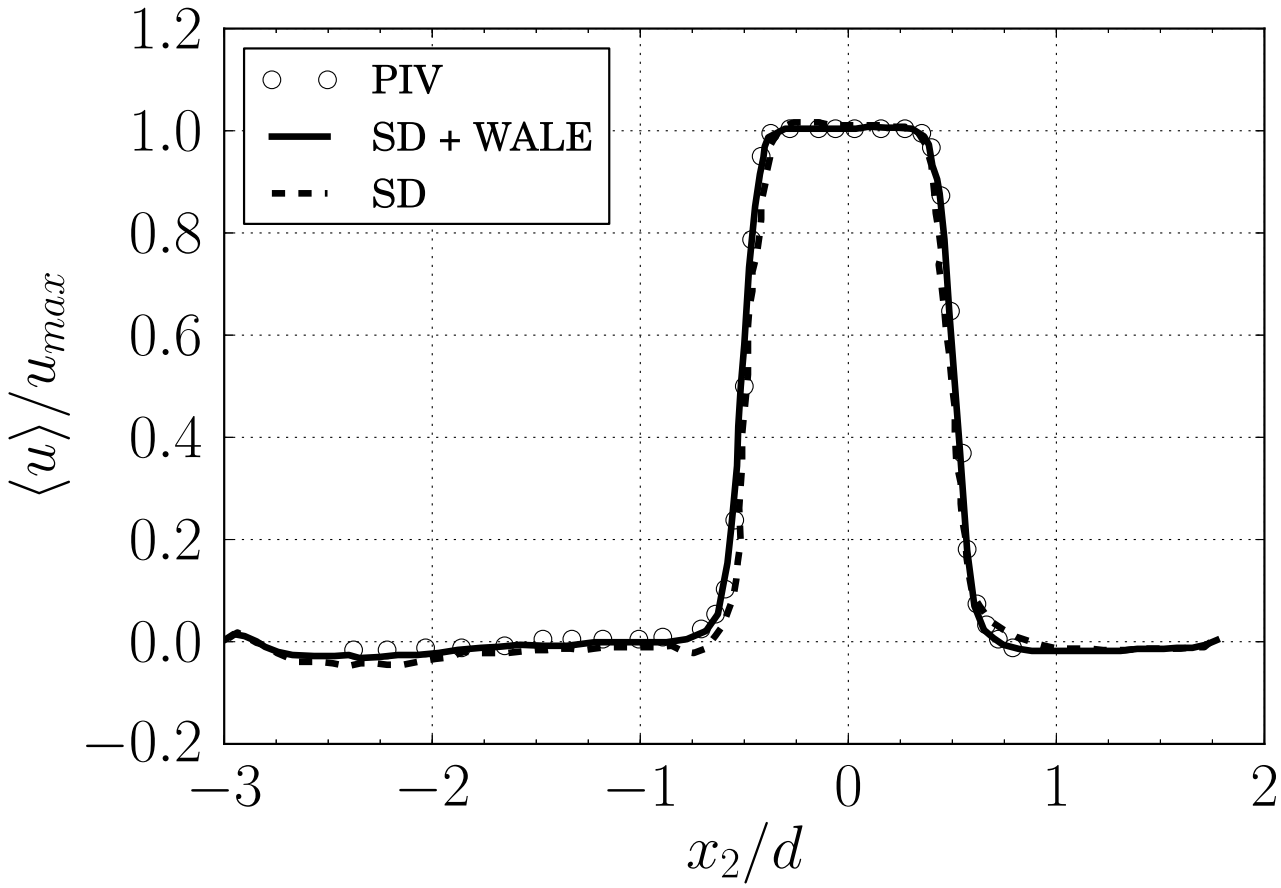

Figure: Time averaged velocity profiles.

Flow in a muffler

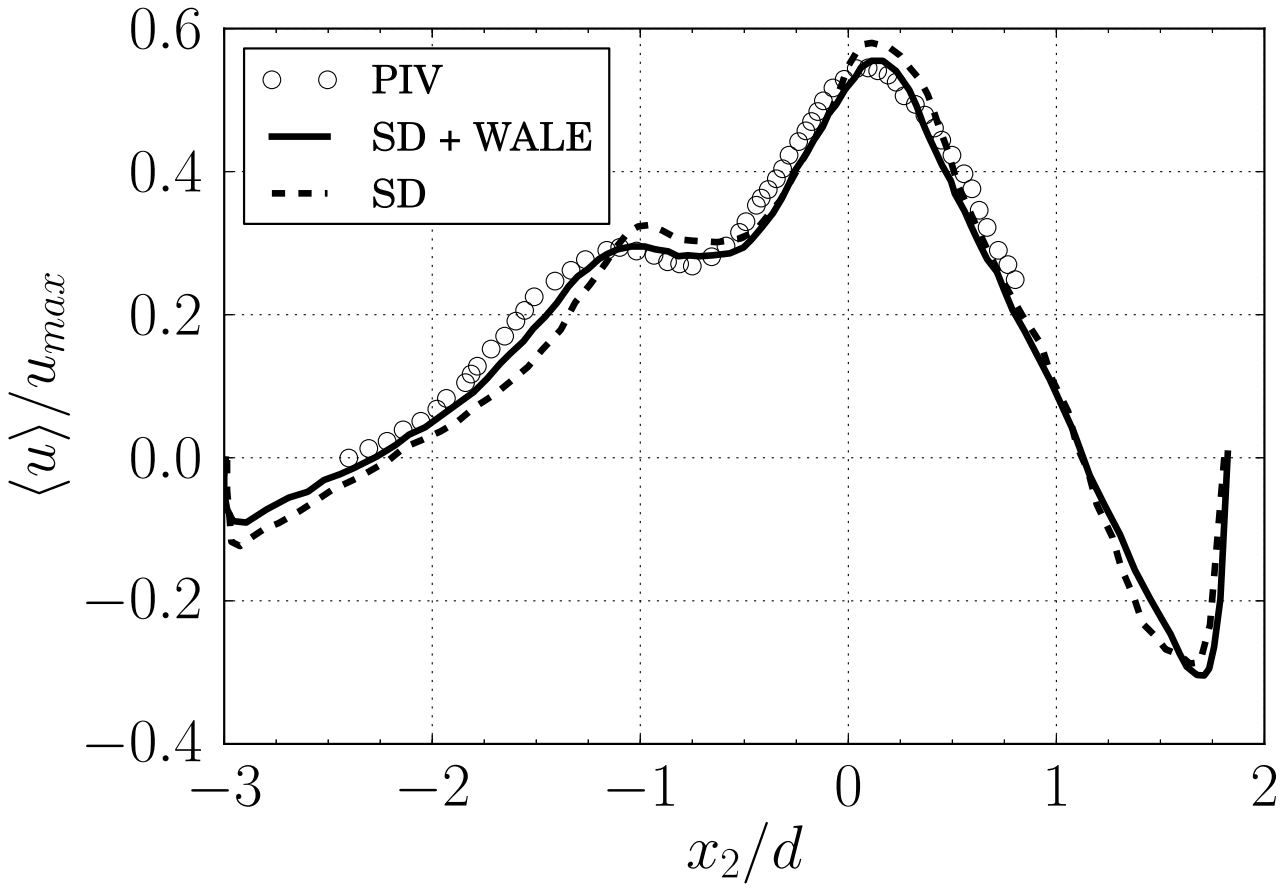

Figure: Time averaged velocity profiles.

Flow in a muffler

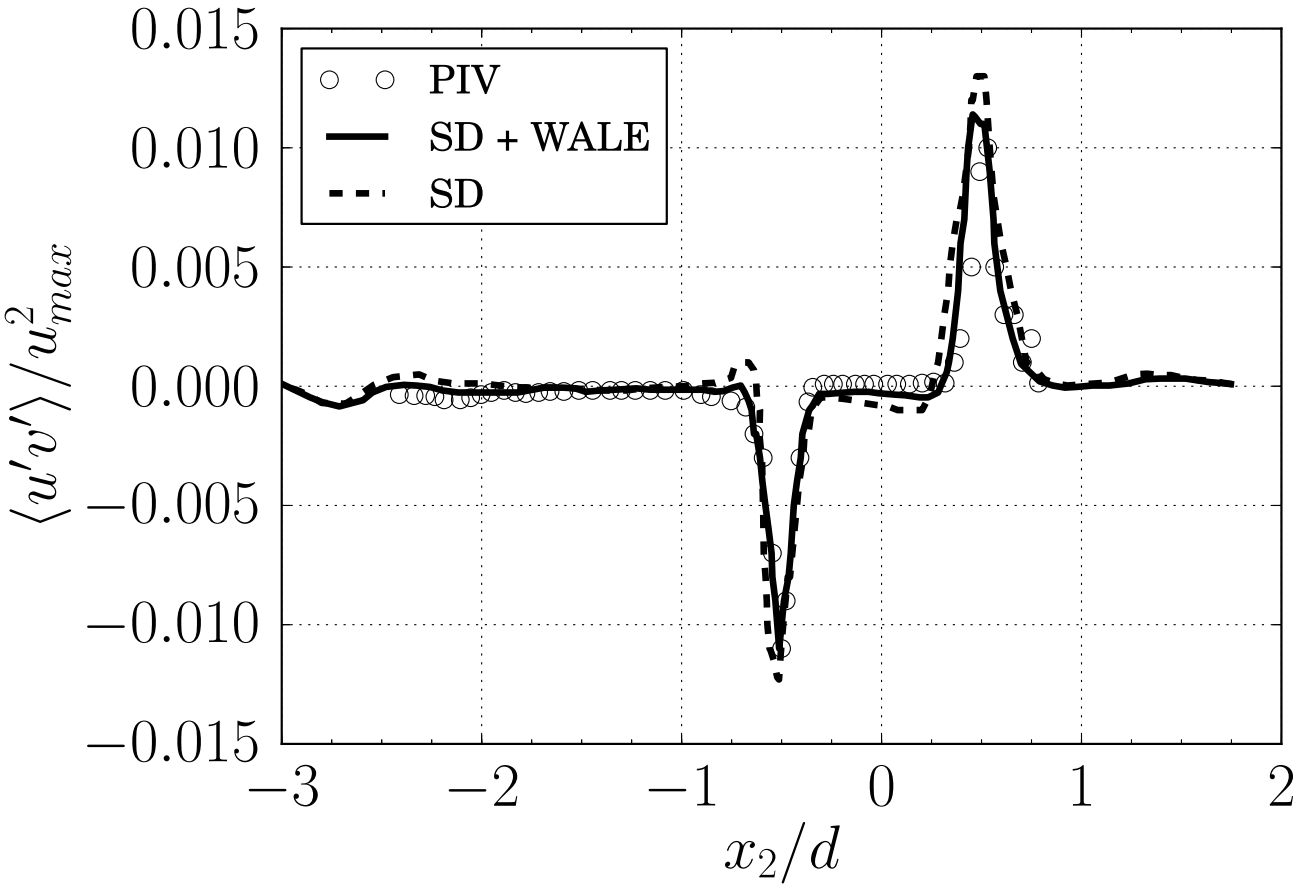

Figure: Reynolds stress.

Flow in a muffler

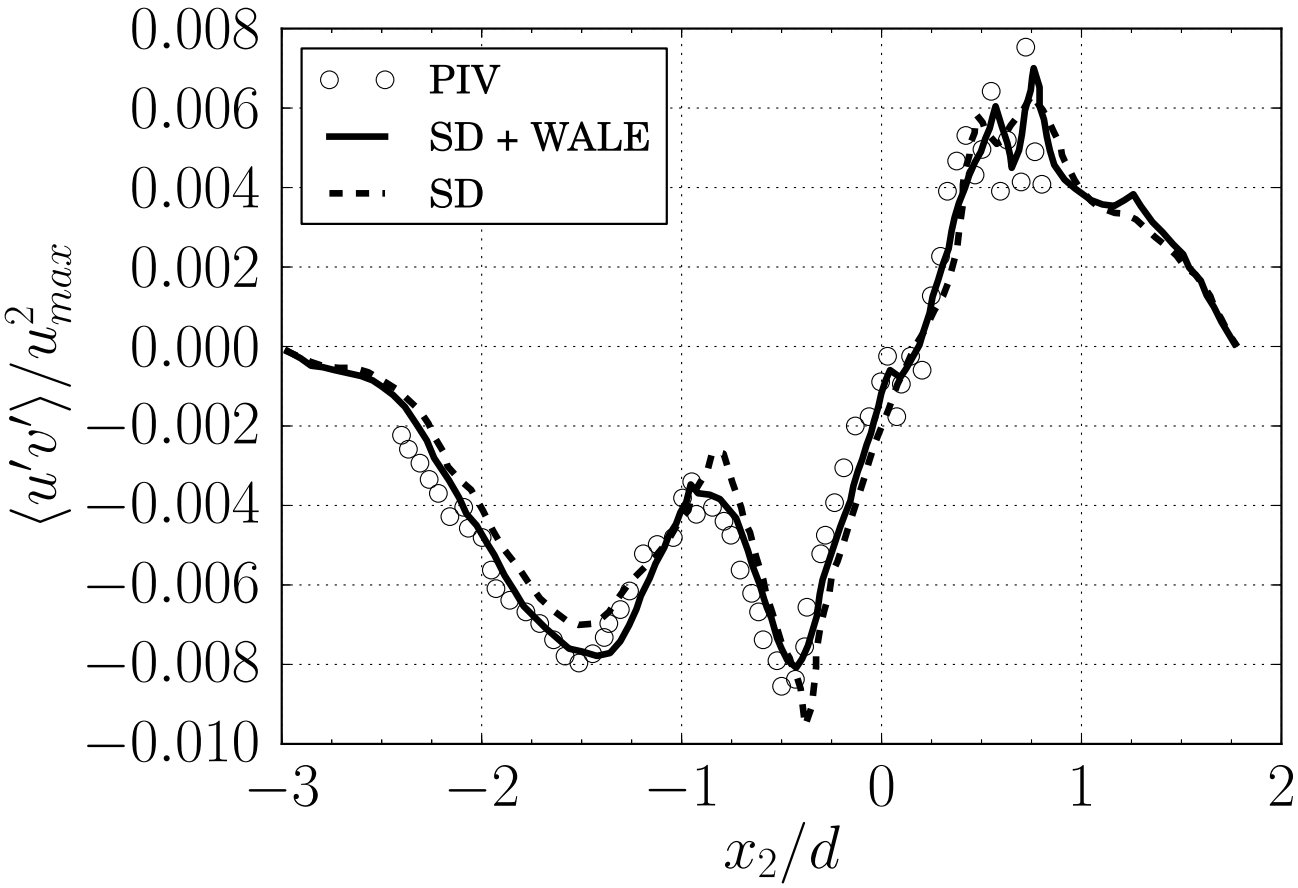

Figure: Reynolds stress.

Conclusions

- Design of **more robust** and **efficient** tailored explicit RK for SD:
  - Linear properties
  - Minimization of the leading truncation error constant
  - Low-storage form with 3 registers
- Numerical verification on unstructured grids
- New schemes are effectively with unstructured grids at CFL_{max}
- Stability efficiency **improvements of** 42% **to** 65%
- No significant sacrifices in accuracy (SD error dominates)
- Extension of the procedure to viscous laminar and turbulent flows is satisfactory (work in progress)
- Etension to embedded Runge–Kutta pair in the very near future

Thank you for your attention!